



ALMA MATER STUDIORUM
UNIVERSITÀ DI BOLOGNA

ARCHIVIO ISTITUZIONALE
DELLA RICERCA

Alma Mater Studiorum Università di Bologna Archivio istituzionale della ricerca

A changepoint analysis of spatio-temporal point processes

This is the final peer-reviewed author's accepted manuscript (postprint) of the following publication:

Published Version:

A changepoint analysis of spatio-temporal point processes / Altieri, L; Scott, E. M; Cocchi, D; Illian, J. B.. - In: SPATIAL STATISTICS. - ISSN 2211-6753. - STAMPA. - 14:Part B(2015), pp. 197-207. [10.1016/j.spasta.2015.05.005]

Availability:

This version is available at: <https://hdl.handle.net/11585/524155> since: 2015-12-13

Published:

DOI: <http://doi.org/10.1016/j.spasta.2015.05.005>

Terms of use:

Some rights reserved. The terms and conditions for the reuse of this version of the manuscript are specified in the publishing policy. For all terms of use and more information see the publisher's website.

This item was downloaded from IRIS Università di Bologna (<https://cris.unibo.it/>).
When citing, please refer to the published version.

(Article begins on next page)

This is the final peer-reviewed accepted manuscript of:

Altieri L, Scott EM, Cocchi D, Illian JB. A changepoint analysis of spatio-temporal point processes. *Spat Stat.* 2015;14:197-207. doi:10.1016/j.spasta.2015.05.005

The final published version is available online at:

<https://doi.org/10.1016/j.spasta.2015.05.005>

Rights / License:

The terms and conditions for the reuse of this version of the manuscript are specified in the publishing policy. For all terms of use and more information see the publisher's website.

This item was downloaded from IRIS Università di Bologna (<https://cris.unibo.it/>)

When citing, please refer to the published version.

8 **Abstract**

9 This work introduces a Bayesian approach for detecting multiple unknown change points over time
10 in the spatially inhomogeneous intensity of a spatio-temporal point process with spatial and temporal de-
11 pendence within segments. We propose a new method for detecting changes by fitting a spatio-temporal
12 log-Gaussian Cox process model using the computational efficiency and flexibility of INLA, and stu-
13 dying the posterior distribution of the potential changepoint positions. In this paper, the context of the
14 problem and the research questions are introduced, then the method is presented and discussed in detail.
15 A simulation study assesses the validity and properties of the proposed method, before the approach is
16 applied to examine potential unknown change points in the intensity of radioactive particles found on
17 Sandside beach, Dounreay, Scotland.

18 **Acknowledgements**

19 The authors would like to thank . . .

1 Introduction

With this work, we aim at proposing a method for carrying out a changepoint analysis in the complex context of spatio-temporal point processes. Our study is motivated by questions on the monitoring and recovery of radioactive particles from Sandside beach, North of Scotland, due to the presence of a former nuclear reactor ?; the distribution of the particles and their behaviour over time in the offshore and foreshore areas are of interest for cleaning purposes. Over the past 15 years, two major changes in the equipment used to detect the particles have taken place, representing known potential change points. In addition, offshore particle retrieval campaigns are believed to have reduced the particle intensity for particles moved onshore with tides and currents with an unknown temporal lag, potentially generating multiple unknown change points in the intensity function. Questions on how to build a method able to detect changepoints in such a complex dataset are raised; the proposed method has to deal with the issues of spatial inhomogeneity, spatial dependence among points and temporal dependence of the process.

1.1 Theoretical issues

Changepoint analysis is a well-established area of statistical research, frequently applied in a temporal context, and less frequently over space. While some of the existing changepoint methods can potentially be extended to the general spatio-temporal context, for spatio-temporal point processes this branch of analysis appears to be as yet relatively unexplored.

The basic assumption in a changepoint analysis is that data are ordered and split into segments, following the same model but under different parameter specifications ?. The other common assumption is that observations are *i.i.d.*. The aim of our work is to propose a method to find change points even when the mentioned assumptions do not hold. Modelling dependence within data segments in the context of unknown multiple change points is currently a challenge, and there is a need for fast approximate methods such as Integrated Nested Laplace Approximation (INLA), an alternative, computationally efficient approach to MCMC methods to obtain the posterior distribution of both the number of change points and their positions [ref]. The computational speed and flexibility of INLA has not been exploited for a spatio-temporal changepoint analysis yet.

Some substantial differences with regard to the standard changepoint analysis in time or in space have to be taken into account: firstly, an individual datum is not a single point but a pattern of points; secondly, the measured response variable is the point location. Frequently, point process data are collected over space, and it is not usual to have repeated measurements on the same observation window over time, in a number large enough to make a changepoint analysis sensible. Nevertheless, most of the studies on point processes aim at describing the behaviour of the intensity function, therefore its changes over time are certainly of interest, and the provision of tools for changepoint analysis on spatio-temporal processes

would enlarge the number of questions that can be answered. Furthermore, in this context both the issues of spatial dependence among points and of temporal dependence within time segments have to be faced, which add further complexity to the analysis.

We do not have knowledge of a changepoint analysis carried over a spatio-temporal point process with recently developed techniques. For all the mentioned reasons, we believe a statistical analysis of changepoint detection methods in the context of spatio-temporal point processes is a challenging and interesting study area.

1.2 Background

To our knowledge, the issue of dependence between data in a changepoint analysis has only been faced with Bayesian methods so far. Fearnhead (2006) proposes a method for simulating from the posterior distribution of multiple changepoints using a recursive technique that should theoretically extend to dependent data; when dependence is allowed, though, the segment marginal likelihood required by Fearnhead’s method usually becomes intractable. Including any type of dependence increases the computational complexity of the problem, and fast methods providing an accurate and tractable approximation of the likelihood even in complex situations have to be developed. Recent work by Wyse, Friel and Rue ? extends the method to allow for dependence within segments, using Integrated Nested Laplace Approximation ? to face the well known difficulty in analytically obtaining the posterior distribution of the parameters. The authors combined recursive methods with INLA, to produce estimates for the segment marginal likelihoods, and approximations for the posterior of both the number of changepoints and their position.

Our work is set in the context of spatio-temporal log-Gaussian Cox point processes (LGCPs). Cox processes assume the point distribution over space (and potential aggregation) is due to stochastic environmental heterogeneity, modelled as a random intensity function $\Lambda(s)$?; given $\Lambda(s)$, the distribution of points follows a inhomogeneous Poisson process. In LGCPs the logarithm of the intensity surface over an observation window W is assumed to be a Gaussian (latent) field $Z(s)$, i.e. $\Lambda(s) = \int_W \lambda(s) ds = \exp(Z(s))$, and conditional on $Z(s)$ the number of points $X \sim Poi(\Lambda(s))$. LGCPs constitute a very flexible class of models that can be extended to the spatio-temporal case and implemented using INLA ?. The INLA approach has several fundamental advantages: above all, it is an effective computational tool for model implementation; this is fundamental in our context as the dataset is very complex (every single datum is a point pattern), therefore computations easily become very slow and demanding. Moreover, the efficiency of INLA allows an extension from the temporal to the spatio-temporal context; furthermore, the likelihood values resulting from different changepoint positions can be evaluated, and a posterior distribution can be approximated to choose the best change-point position a posteriori.

We address the analysis of temporal change points in a spatially inhomogeneous intensity function defi-

87 ning a point process observed over a window. An approximate likelihood based methodology is develo-
 88 ped to detect change points and obtain estimates of the two-dimensional intensity function at each time
 89 point. We present a simulation study of this approach in the spatio-temporal point process context; unlike
 90 traditional changepoint detection algorithms (see ?), with this method the 3 dimensions of the problem
 91 (two spatial and one temporal) are maintained. We propose two different Bayesian techniques allowing
 92 decisions on whether, how many and when temporal change points occur.

93 2 Methodology

94 2.1 Models

95 We define a change point under four increasingly complex point process models, and consider the
 96 case of both a single changepoint and multiple change points at unknown locations; we discretise the
 97 observation window into a fine grid, and define $y_{ts} \sim Poi(|C|\lambda_{ts})$ as the number of points at time $t =$
 98 $1, \dots, T$ in cell $s = 1, \dots, S$, where $|C|$ is the cell area. We initially consider a model with a fixed effect
 99 which assumes a spatially homogeneous intensity λ_t ; under each hypothesis (for the alternative, the
 100 simple case of a single change point is displayed) we model the logarithm of the intensity function λ as:

$$\begin{aligned} H_0: \quad \log(\lambda_t) &= \mu + \varepsilon_t & \text{for } t = 1, \dots, T \\ H_1: \quad \log(\lambda_t) &= \mu_1 + \varepsilon_t & \text{for } t < \tau^* \\ &= \mu_2 + \varepsilon_t & \text{for } t \geq \tau^* \end{aligned} \quad (1)$$

101 where μ is the fixed effect and ε is an unstructured error term. Under H_0 all values over both space and
 102 time depend on a single value for μ , while under H_1 μ_t is constant over space but allowed to vary over
 103 time. Note that a single change point in location τ^* splits the dataset into two time segments with a
 104 different value for the intensity function (i.e. two equations under the alternative hypothesis), so for a
 105 single change point we first have to detect where the change occurs, and then we estimate two values for
 106 μ . In the more general case of $M \geq 2$ change points, the equation under H_1 is split into $M + 1$ segments,
 107 time intervals defined by the ordered changepoint locations $\tau_1, \tau_2, \dots, \tau_M$. Note that each changepoint
 108 position $\tau_m, m = 1, \dots, M$, corresponds to the first point of a new segment.

109 The second model adds a temporal effect:

$$\begin{aligned} H_0: \quad \log(\lambda_t) &= \mu + \phi + \varepsilon_t & \text{for } t = 1, \dots, T \\ H_1: \quad \log(\lambda_t) &= \mu_1 + \phi_1 + \varepsilon_t & \text{for } t < \tau^* \\ &= \mu_2 + \phi_2 + \varepsilon_t & \text{for } t \geq \tau^* \end{aligned} \quad (2)$$

110 and within each time segment ϕ is a random effect modelled as an AR(1), i.e. the logarithm of the
 111 intensity function at every time point is supposed to depend on its own value at the previous time. Hy-
 112 perparameters are needed for the precision $\tau_\phi \sim Gamma(\alpha_\phi, \beta_\phi)$. Other time dependence structures can

113 be easily modelled using INLA.

114 The first two models both consider a spatially homogeneous intensity function, therefore there is no spa-
 115 ce index s because at each time point the intensity takes a single value over the window. We now allow
 116 the intensity to vary over space as well as over time, and build a model with a spatial effect:

$$\begin{aligned}
 H_0 : \quad \log(\lambda_{ts}) &= \delta + \psi_s + \varepsilon_{ts} & \text{for } t = 1, \dots, T \text{ and } s = 1, \dots, S \\
 H_1 : \quad \log(\lambda_{ts}) &= \delta + \psi_{1s} + \varepsilon_{ts} & \text{for } t < \tau^* \text{ and } s = 1, \dots, S \\
 & \log(\lambda_{ts}) = \delta + \psi_{2s} + \varepsilon_{ts} & \text{for } t \geq \tau^* \text{ and } s = 1, \dots, S
 \end{aligned} \tag{3}$$

117 where δ is a common intercept and ψ_s describes spatial dependence; it is indexed by s as we assume
 118 that the basic space unit is the grid cell, and that the intensity function is constant inside the cell. This
 119 approximation is needed for tractability reasons, but thanks to INLA we can build as fine a grid as we
 120 wish without encountering computational issues, so that the approximation error is very low and can be
 121 controlled. Under H_1 , a single value defines the intensity for each cell over all the time segment, and
 122 after the change point the value for each cell changes. The spatial effect is modelled as an intrinsic CAR,
 123 i.e. as a Random Walk in two dimensions on a lattice; the model is easily specified with INLA, with a
 124 neighbourhood structure that gives non-zero (decreasing) weights to the first 12 neighbours in the lattice.
 125 This produces a very smooth spatial structure which is suitable for LGCPs, where the hypothesis is that
 126 there is a smooth underlying driver defining the intensity function. Again, the precision hyperparameter
 127 can be defined as $\tau_\psi \sim \text{Gamma}(\alpha_\psi, \beta_\psi)$.

128 For the fourth, most complicated model we consider an offset term, a temporal effect and a spatial effect,
 129 allowing for spatially inhomogeneous intensity:

$$\begin{aligned}
 H_0 : \quad \log(\lambda_{ts}) &= \delta + \phi + \psi_s + \varepsilon_{ts} & \text{for } t = 1, \dots, T \text{ and } s = 1, \dots, S \\
 H_1 : \quad \log(\lambda_{ts}) &= \delta + \phi_1 + \psi_{1s} + \varepsilon_{ts} & \text{for } t < \tau^* \text{ and } s = 1, \dots, S \\
 & \log(\lambda_{ts}) = \delta + \phi_2 + \psi_{2s} + \varepsilon_{ts} & \text{for } t \geq \tau^* \text{ and } s = 1, \dots, S
 \end{aligned} \tag{4}$$

130 Please remember that in these models the temporal dependence is only assumed to be within, not across,
 131 segments. The precision parameter for both temporal and spatial effects has a *Gamma* prior that is by
 132 default set as non-informative but can be tuned according to a specific context.

133 When looking for a single change point, each model is run one time for every possible changepoint
 134 position, i.e. for every time point with a non-zero prior probability of being a change point. By fitting
 135 every model with INLA, a series of likelihood values is then produced, and normalised (in absence of
 136 prior knowledge) to obtain the posterior distribution of the change points: this gives, for every time
 137 point, the posterior probability of being a change point. Once the posterior is produced, methods for
 138 identifying significant change points are proposed in Section 2.2. Since each model is run many times
 139 assuming different changepoint positions, there is a need for efficient computational tools in order to
 140 obtain results in a reasonable time, and that is one of the reasons why we fit the models using INLA.

141 The approach for detecting multiple unknown change points is described in Section 2.3.

142 2.2 Changepoint detection methods

143 We propose two different Bayesian techniques for assessing the presence of change points.

144 The first option derives from the Bayes Factor, used in absence of prior knowledge to decide if there is a
145 change point ?. The Bayes Factor can be written as

$$\gamma = \frac{\sum_{\tau} \pi(\tau) Q_1(\tau) Q_2(\tau)}{L_0} \quad (5)$$

146 where $Q_1(\tau)$ and $Q_2(\tau)$ are the segment maximum likelihood values, i.e. the maximum likelihoods for
147 the two segments resulting from a changepoint position in $\tau \in \{1, \dots, T\}$; for every value of τ , a pair of
148 values $Q_1(\tau)$ and $Q_2(\tau)$ is returned. Besides, $\pi(\tau)$ is the prior probability of the time point τ of being a
149 change point, and L_0 is the likelihood value obtained by running the model once under H_0 .

150 The Bayes Factor expresses the evidence showed by data in support of the alternative model with regard
151 to the null model. Since independence across segments is assumed, for every changepoint position the
152 maximum likelihood value under the alternative hypothesis is $L_1(\tau) = Q_1(\tau) Q_2(\tau)$. The formula (5) can
153 be extended to the case of a non-vague prior distribution by taking the posterior ratio, i.e. the product of
154 likelihoods and prior ratios.

155 The prior weight $\pi(\tau)$ in the nominator sum shrinks each alternative likelihood value, still every element
156 in the sum will be positive, and the greater the nominator is, the more likely it is to reject H_0 . We choose
157 a more conservative condition, by substituting the sum in the numerator with a single term:

$$\gamma_{\tau^*} = \frac{\pi(\tau^*) Q_1(\tau^*) Q_2(\tau^*)}{L_0} = \frac{\pi(\tau^*) L_1(\tau^*)}{L_0} \quad (6)$$

158 where τ^* is the most likely changepoint position, i.e. the one returning the highest likelihood value
159 under H_1 , $\pi(\tau^*)$ is the prior distribution on its position, and $L_1(\tau^*)$ is the maximum likelihood under the
160 alternative hypothesis: a value for the likelihood is obtained for every potential changepoint position τ ,
161 the highest one is chosen and the corresponding location is the τ^* to test. Equivalently, we can take the
162 logarithm of (6)

$$\gamma'_{\tau^*} = \log(\pi(\tau^*)) + q_1(\tau^*) + q_2(\tau^*) - l_0 = \log(\pi(\tau^*)) + l_1(\tau^*) - l_0. \quad (7)$$

163 For the model with no change points, the maximum log-likelihood value under H_0 is greater than the
164 maximum log-likelihood value under H_1 , therefore the absolute threshold for this statistic, irrespective
165 of the model used, is zero. Indeed, differently from the frequentist likelihood ratio, when using the Bayes
166 Factor models with more parameters do not necessarily produce higher likelihood values, as Bayes fac-
167 tors naturally incorporate penalization for model complexity, so there is no need for an extra penalization
168 term as in AIC or SIC. If $\gamma'_{\tau^*} > 0$, we reject the null model of no change points, and the change point is
169 estimated to occur at τ^* .

171 An alternative option we propose is another typical Bayesian way of taking decisions, i.e. by looking
172 at the posterior distribution and fixing a posterior probability threshold for significant values: once the
173 resulting curve is plotted, a threshold value is fixed in order to take decisions on which time points are to
174 be considered change points.

175 As for the threshold choice, it is to bear in mind that greater values (closer to 1) will lead to more
176 conservative conclusions, and smaller values (closer to 0) will detect change points more easily. Hints
177 for discussion on the choice of the threshold are given in Section 5. This method has the advantage
178 of being visually immediate and easy to explain to non-statisticians; moreover, it is very flexible as the
179 threshold choice can be adapted to the model fitting the data and to the analysis context. In the special
180 case of a known changepoint position to test, the method does not change: a posterior probability curve
181 will be estimated all the same, and the threshold will be only used to evaluate the significance of that
182 specific changepoint position.

183 **2.3 Binary segmentation algorithm**

184 Both the models presented in Section 2.1 and the detection methods presented in Section 2.2 refer
185 to a single changepoint search. The method can be extended to a multiple unknown number of change
186 points, the most complicated type of changepoint analysis. The hypotheses become:

187 H_0 : no change points

188 H_1 : ≥ 1 change points.

189 As for the single changepoint detection, note that H_1 is not bound to a specific changepoint position; the
190 alternative hypothesis is very complex because it considers the presence of change points first, but then
191 the number and positions also have to be estimated. If H_0 is rejected, $\tau^* = (\tau_1^*, \dots, \tau_M^*)$ is a $M \times 1$ vector
192 containing the estimated changepoint positions, a subset of $(1, \dots, T)$.

193 The simplest and most straightforward way of running a multiple changepoint analysis is to use a binary
194 segmentation method. For a general introduction to these methods we refer to [killickeckley], and in
195 particular for point processes to the work by [park2012]. An alternative option would be to perform a
196 simultaneous changepoint search; this method is discarded as, with our techniques, it proved to perform
197 poorly as it tends to underestimate the number of change points: different change points will refer to
198 changes of different magnitudes in the intensity function; when the posterior probability curve is nor-
199 malised, posterior peaks will tend to flatten, and changepoint positions corresponding to smaller, but not
200 negligible, changes happen to be considered non-significant. A binary segmentation algorithm allows to
201 find local maxima and has proved itself better performing in our analysis.

202 The idea of a binary segmentation procedure, and the key to its simplicity, is to split the multiple search
203 into a series of subsequent single changepoint searches. It is an iterative procedure, which in general can
204 be structured into steps:

- 205 1. Run a changepoint analysis on the whole data series Y , testing the simple hypotheses
- 206 H_0 : no change points
- 207 H_1 : one change point.
- 208 2. a) If no change points are found, stop the algorithm.
- 209 b) If one change point is found, its position is defined as τ_0^* , and data are split in correspondence
- 210 of τ_0^* into two segments, Y_A ($[S \times (\tau_0^* - 1)] \times 1$) and Y_B ($[S \times (T - \tau_0^* + 1)] \times 1$). For each of the two
- 211 resulting segments, go back to step 1.
- 212 3. a) If no more change points are found, the dataset has a single change point in τ_0^* .
- 213 b) If change points τ_A^* and/or τ_B^* are detected, go back to step 2b and repeat the procedure for each
- 214 segment containing a change point.
- 215 4. Repeat until either no more change points are detected in any segment, or a pre-fixed number of
- 216 change points is reached, or a minimum segment length is reached for all segments.

217 Many binary segmentation methods can be built, according to the criterion for detecting a change point

218 and to the criterion for stopping the search; what they have in common is that at each step the algorithm

219 runs a single changepoint search for every segment. Intuitively, the analysis can become computatio-

220 nally very demanding as T and M become large, and methods are available for reducing time and me-

221 mory storage requirements [ref needed]. This is nevertheless the general idea we follow, and again the

222 computational efficiency of INLA makes this algorithm feasible even for such complex spatio-temporal

223 data.

224 3 Simulation study

225 3.1 Simulation design

226 In order to assess and compare the performance of the two methods proposed in Section 2.2, we carry

227 out a simulation study covering different situations. We fix a time series of $T = 50$ time points, and a

228 grid of $S = 20 \times 20 = 400$ cells. The observation window is a square of area 100 and the initial intensity

229 value is $\lambda = 1$, generating 100 points on average in the window. We allow for spatial inhomogeneity: the

230 value for λ gives the average number of points at each time point, but the spatial structure changes over

231 the window. More precisely, we build a smooth spatial trend which is stronger in the top-right corner and

232 then progressively decreases toward the bottom-left corner (see Fig.1 for an example before and after the

233 change point). We build the series assuming that the spatial structure is the same over time up to a scale

234 parameter, and the changepoint detection identifies the time point that corresponds to the change of scale

235 in our data.

236 We generated both iid and AR(1) data series, under the hypotheses of no change point, one change point
237 and three change points. For the single changepoint series, we tried two different change magnitudes: a
238 big one, from $\lambda_1 = 1$ to $\lambda_2 = 2$, and a small one, from $\lambda_1 = 1$ to $\lambda_2 = 1.2$. As for the multiple changepoint
239 series, we set two positive changes and a negative one: the segment intensity values are $\lambda_1 = 1$, $\lambda_2 = 1.4$,
240 $\lambda_3 = 2.3$ and $\lambda_4 = 2$. The last change is extremely small, to further test the performance of the detection
241 methods. Each one of these time series was replicated 100 times. A summary of the simulation design is
242 in Fig. 2.

243 Both iid and time dependent data are generated as their behaviour is very different for what concern
244 change points. Fig. 3 shows some time series made by counting the number of points for each time
245 point. As it can be seen, iid data keep very close to the initial set value over the series, and the change
246 points are easily recognizable. On the contrary, AR(1) data tend to drift far away from the initial value,
247 and are far more variable. On one hand, this can result in the detection of spurious change points, i.e.
248 change points that are due to the variability of the series and not to external factors; on the other hand
249 changes set in the simulation may not be identifiable. It is therefore of interest to test the methods on
250 both types of data.

251 On all the generated time series we fit the four models described in Section 2.1 and try to detect change
252 points with both methods described in Section 2.2. All model fitting is done using INLA.

253 3.2 Simulation results

254 The two methods' performance was evaluated according to type I and type II errors, number and
255 position of detected change points and values of the intensity estimates.

256 As for the errors, a summary of the performance is in Fig. 4. In general, the Bayes Factor method
257 performs very well as regards the first two models: in most cases type I errors are very small (with the
258 exception of one case with time dependent data, but we expect poorer performance on these data, for
259 the reasons introduced in Section 3.1) and type II errors are negligible in all cases. When we fit more
260 complicated models including spatial effect, though, the performance is very poor: the method is too
261 conservative and does not detect change points, irrespective of their magnitude.

262 The posterior threshold method holds a better performance over all models; this is sensible, as the th-
263 reshold value can be tuned according to the model. A few 'grey' zones are produced, but the overall
264 conclusions are correct in most cases, and there is at least some ability to detect changes in all situations.

265 A further summary of this performance can be found in Fig. 5: the first row in each table concerns data
266 generated under H_0 and the second row concerns data generated under H_1 , therefore numbers have to
267 sum to 100 by row. It is very plain that the PT method has a better overall performance: as regards null
268 data (first row), the behaviour of the two methods is very similar, but the PT method is 20 percentage
269 points better in finding change points in H_1 data (second row).

270 As for the number of detected change points, results are linked, but not necessarily identical, to the pre-
271 vious results: committing or not a type II error only concerns the rejection of H_0 and tells nothing on
272 the number and positions of change points found, which is of special interest in the multiple changepoint
273 search. Fig. 6 shows a summary of the results. We can see that as far as H_0 data are concerned, results
274 are correct in all cases: even in situation where some change points were found, as in AR(1) data, all
275 the positions were different, and this indicates they are spurious change points and not 'true' ones. As
276 regards the detection in H_1 data, the BF method suffers from the above mentioned issue: it is very precise
277 in detecting the true change(s) in the first two models, but is too conservative when spatial dependence
278 and inhomogeneity is introduced. The PT method performs much better: when change points are not
279 detected in the majority of replicates, it is due to the small magnitude of the change, which means the
280 method is not too sensible; despite the small size, a percentage of replicates still had a change detected.
281 The only wrong conclusion concerns the multiple changepoint iid data series under the most complicated
282 model; in all other cases, conclusions are very sensible and the detected position are correct or as close
283 as makes no difference. It is interesting to note that spurious changes in the time dependent data do not
284 affect the conclusions.

285 Lastly, a few comments about the intensity estimates, which again depend on the above presented resul-
286 ts. A summary of the estimated values is given in Fig. 7. Note that the intensity is a inhomogeneous
287 function which takes different values over space. In this table, for brevity reasons, only the mean value
288 is reported, but the mean range (over the replicates) and credibility bands are also available. Given the
289 detected change points, estimates are very accurate over all the simulated scenarios: when a change point
290 was not detected, values are an average between the two segments' true values, and when a change point
291 was only detected in part of the replicates (as it happens with very small changes), the true magnitude of
292 the change is shrunk. In all cases the correct (increasing or decreasing) trend is captured. It is possible
293 to see an example of the produced estimates in Fig. ??: it represent a multiple changepoint data series,
294 where the above panels show the true values for the intensity in the four segments, and the below panels
295 show the three segments estimated by INLA, after detecting two change points (the last change has a
296 very small magnitude and was not detected).

297 After assessing the performance of the methods, we applied both of them to the motivating dataset.

298 **3.3 Extension: changes in the spatial structure**

299 All the simulated data series are generated taking a constant spatial structure for the intensity function
300 and allowing for a change in scale, i.e. a change point corresponds to a greater or smaller number
301 of points in the window, which follow the same spatial distribution. We are interested in relaxing the
302 assumptions and allowing the intensity function to change in space as well, as it happens in many real
303 situations. This might lead to two different types of change: a change in structure, when the overall

304 number of points remain approximately the same but the spatial distribution changes, and a change in
305 both scale and structure.

306 We believe our methods hold over this general situation as well: when looking for a change with the
307 proposed algorithms, we never specify that we are looking for a different number of points. We try
308 and split the data at all different time points and we look for the single equation (no change point) or
309 $M + 1$ equations (M change points) that describe the dataset best, irrespective of the type of change that
310 occurred. Therefore, if we use a model that includes a spatial effect, we expect our methodology to be
311 able to identify change points in both space and time.

312 For studying this situation, we only worked on inhomogeneous data generated under the alternative
313 hypothesis of one change point. The spatially homogeneous case is of no interest here, and if the method
314 works for a single changepoint search it is straightforward to extend it to multiple changes. We used
315 the same values for T , S and W and the change point is again set in the centre of the time series. We
316 cover both cases of only spatial change and spatial plus scale change. An example of generated data can
317 be seen in Fig 8. As expected, results are very good and show that the methods are able to detect all
318 types of change. A summary of the performance of the methods in terms of power is displayed in Tab
319 9. As expected, the first two models do not perform very well in detecting a spatial change (yellow area
320 in the table), as the spatial effect is not included and they assume the intensity function is constant over
321 time. There are no substantial differences in the performance of the BF and PT method. It is nevertheless
322 interesting to point out that, in the minority of cases where the change point is detected, it is in the correct
323 location.

324 The spatial and scale change is correctly detected in all replicates even in the homogeneous models, as a
325 change in the number of points is recognized as change point over all models.

326 The most interesting result is that, as soon as the spatial effect is included (model 3 and 4), conclusions
327 are perfectly correct. The BF method performs even better than in the only-scale change situation, as it
328 does not suffer from too much conservatism.

329 The INLA estimates, again, reproduce very accurately both the scale and the spatial structure of the time
330 segment intensity function in all cases.

331 **4 Particle data**

332 Since the 1950s, Dounreay has been the site of several nuclear research establishments, because of
333 its isolation for safety reasons. In 1994, the last reactor ceased operation and the area is currently being
334 decommissioned (<http://www.dounreay.com>). Radioactive particles have been found on local beaches in
335 the North of Scotland since the 1990s as a result of historic practices during nuclear fuel reprocessing at
336 the Dounreay plant. The data set used gives the particles' locations on one of the local beaches, Sandside

337 beach, during each of the years of monitoring. The temporal data series is made of yearly point pattern
 338 realizations, and additional information about the retrieval and radioactivity level also labels each particle
 339 once it has been collected and examined. The underlying intensity and its spatial structure are of interest,
 340 along with potential changes in its strength. The dataset presents some difficulties when a changepoint
 341 analysis is carried out: the time series is not long ($T = 15$) and some yearly patterns present very few
 342 points. Still, the questions are of interest, and the method performance has already been tested over
 343 simulated data.

344 An exploratory analysis shows that Cox processes fit data very well; in particular, the flexible class of
 345 log-Gaussian Cox processes is realistically suitable for the problem as the distribution of particles could
 346 be due to an underlying driver (tides and winds). Moreover, it is very straightforward to complicate these
 347 models by adding fixed, random or smoothed effects to the structured predictor; the estimation with
 348 INLA is very fast (and precise) even for complex models and this allows to try many different models
 349 without high computational effort.

350 4.1 Results on particle data

351 Table 4.1 and 4.1 display a summary of the number and positions of detected change points in the
 352 data series for both a single and a multiple search.

353

Model	Change point (BF)	Change point (PT)
Fixed	2006	2006
Temporal	2003	2003
Spatial	—	2006
Sp-temp	—	—

354

Model	Change point (BF)	Change point (PT)
Fixed	2003, 2006, 2012	2003, 2006, 2012
Temporal	2003	2003, 2006, 2012
Spatial	—	2006, 2012
Sp-temp	—	—

355

356 Results must be interpreted carefully since the time series is very short, but they are sensible given
 357 the context. The first two detected change points correspond to the periods of equipment changes and
 358 produce an increase in the point intensity; this supports that the changes in equipment has significantly
 359 improved the probability of detecting particles. The third change point is very close to the end of the

360 series, therefore conclusions must be drawn with a special care; it gives a hint of a decreasing intensity,
361 which could be related to the offshore retrieval campaign, suggesting a reduction of the arrival of parti-
362 cles on Sandside beach.

363 An example of the analysis output is given in Fig. 10: this shows the result for a multiple changepoint
364 detection using the model including spatial dependence and the Posterior Threshold method. The po-
365 sterior probability plot in the first panel shows that two significant change points have been detected, in
366 2006 and 2012; the right hand side part of the figure shows a comparison between non-parametric kernel
367 estimates and INLA estimates. This dataset is similar enough to the case covered by our simulation
368 study: the spatial structure of the intensity function is inhomogeneous, but can be considered constant
369 over time up to a scale parameter, with a low density value in most of the window and a hot spot in the
370 bottom-right area. The reported scale of values shows that there is a significant increase in the intensity
371 after 2006, and then a significant decrease in the last two years of the series.

372 **5 Discussion**

373 In this work, we presented a new method which is able to find unknown multiple change points in the
374 intensity of a spatio-temporal point process. The novelty of our method lies in the ability of modelling
375 both spatial and temporal dependence on such a complex point dataset.

376 A few considerations can be done on the methodology we follow and the results we obtain.

377 All the models presented in Section 2.1 are very simple, but they contain the key elements for the ana-
378 lysis, i.e. spatial inhomogeneity, spatial dependence and temporal dependence. Once we find a method
379 that allows to detect change points in these situations, it is straightforward to complicate the models by
380 adding fixed effects, such as covariates, and random effects (in a limited number), up to very complex
381 models able to give a good description of many real situations.

382 As for the fitting with INLA, a log-likelihood value is returned for every fitting. What we are interested
383 in, as in all Bayesian inference, is the posterior distribution. In our work, this is simply obtained by
384 normalising the likelihood values, as we set non-informative priors on both number of change points
385 and their positions. According to the specific context, different prior distributions can be set, and the
386 posterior distribution is found by following the general Bayes rule of multiplying prior and likelihood
387 and then rescaling in order to have a proper distribution.

388 As for the threshold choice in the PT method, it is to bear in mind that greater values (closer to 1) will
389 lead to more conservative conclusions, and smaller values (closer to 0) will detect change points more
390 easily. The choice of the threshold can therefore be knowledge-driven, if information is available on the
391 diffusion of change points in the data series. Note that useful knowledge can also be incorporated in
392 the posterior through the prior distribution. Another important notion is that the height of peaks in the

393 posterior distribution depends on the length of the time series: since the curve must integrate to 1, longer
394 T s will flatten its peaks. For example, Park et al. (2012 but CHECK REF!) use a threshold of 0.1 for
395 a data series of $T = 1000$; the same value would certainly lead to the acceptance of too many change
396 points in a shorter series. In order to find a sensible and not too arbitrary threshold h , it is possible to
397 use simulated data under the null hypothesis for assessing the significance level α based on different
398 values of h . Once we find a value for h such that the significance level does not exceed a certain limit
399 (usually $\alpha \leq \{0.01, 0.05, 0.1\}$), we use that threshold on data generated under the alternative hypothesis
400 in order to evaluate its power level, the ability to detect the correct change points and the accuracy of the
401 estimates produced. This is the idea we follow in our simulation study.

402 As for what concerns the results, there are multiple aspects we can focus on. In some changepoint ana-
403 lysis, the interest only lies on where the change point(s) occur(s), and not on the parameter estimates.
404 In many other cases, it is of interest to understand if the change is positive (an increase in the estimated
405 values) or negative (a decrease in the estimated values). For all these cases, the accuracy of the estimates
406 is not the main goal, and a good performing detection method is all that is needed. Nonetheless, we want
407 to focus on the most general case, where the estimate (in our case, the intensity estimate) is of interest
408 and an accurate estimation method is also required, once the change points are detected.

409 The performance of INLA is very satisfactory as regards both computational time and produced esti-
410 mates. Please note that the ability of detecting change points does not depend directly on the INLA
411 approach, but depends on the choice of the detection method: we have seen that the Bayes Factor me-
412 thod and the Posterior Threshold method have different performances, even if they are used on the same
413 model, i.e. they are used on the same set of likelihood values produced by INLA. Given the detection
414 of change points, INLA performs very well in reproducing both spatial trend and scale of values of the
415 intensity function over all the simulation study. Note that the accuracy of INLA is high when the hypo-
416 thesis underlying the use of INLA work: the random field has to be well approximated by a Gaussian
417 field, with a smooth but limited spatial structure (i.e. a sparse covariance matrix for the parameters).
418 As for the computational time, in the simulation study running the models took a few minutes for every
419 replicate, on real data all results were obtained in less than 30 minutes in total. Should computational
420 time issues be encountered, for example if working on an extremely long time series and an extremely
421 dense dataset, there is an alternative to the grid approach, the Stochastic Partial Differential Equation
422 approach (SPDE, see [ref]).

423 This work is a first step toward spatio-temporal changepoint analysis. Many interesting extensions are
424 possible. A further step would be to generalise the intensity function in order to allow its spatial structure
425 to change over time and look for changes in structure as well as scale changes. Looking for improved
426 version of the detection methods would be of interest; Wyse, Friel and Rue (2011) propose a combination
427 of INLA and recursive techniques to look for multiple change points: an extension of this methodology

428 to the spatio temporal case may lead to better result with regard to the Bayes Factor method.

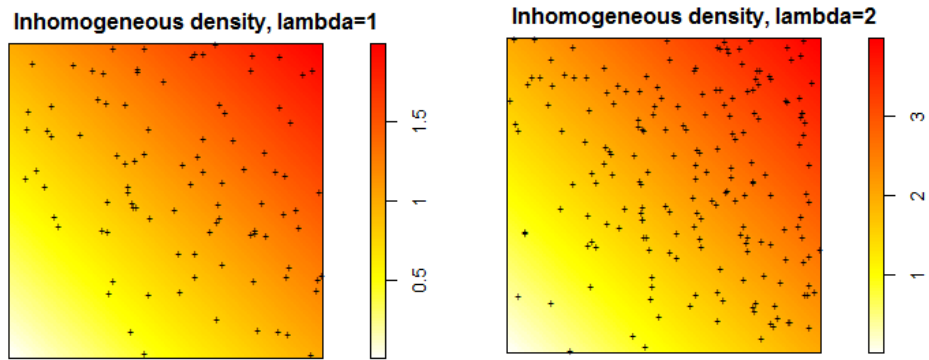


Figura 1: Simulated data - example

			MODEL 1		MODEL 2		MODEL 3		MODEL 4		
			BF	PT	BF	PT	BF	PT	BF	PT	
IID	H ₀	$\lambda=1$	100repl	100repl	100repl	100repl	100repl	100repl	100repl	100repl	100repl
		$\lambda_2=2$	100repl	100repl	100repl	100repl	100repl	100repl	100repl	100repl	100repl
	H ₁	$\lambda_2=1.2$	100repl	100repl	100repl	100repl	100repl	100repl	100repl	100repl	100repl
		multiple	100repl	100repl	100repl	100repl	100repl	100repl	100repl	100repl	100repl
AR(1)	H ₀	$\lambda=1$	100repl	100repl	100repl	100repl	100repl	100repl	100repl	100repl	100repl
		$\lambda_2=2$	100repl	100repl	100repl	100repl	100repl	100repl	100repl	100repl	100repl
	H ₁	$\lambda_2=1.2$	100repl	100repl	100repl	100repl	100repl	100repl	100repl	100repl	100repl
		multiple	100repl	100repl	100repl	100repl	100repl	100repl	100repl	100repl	100repl

Figura 2: Table 1 - Simulation design

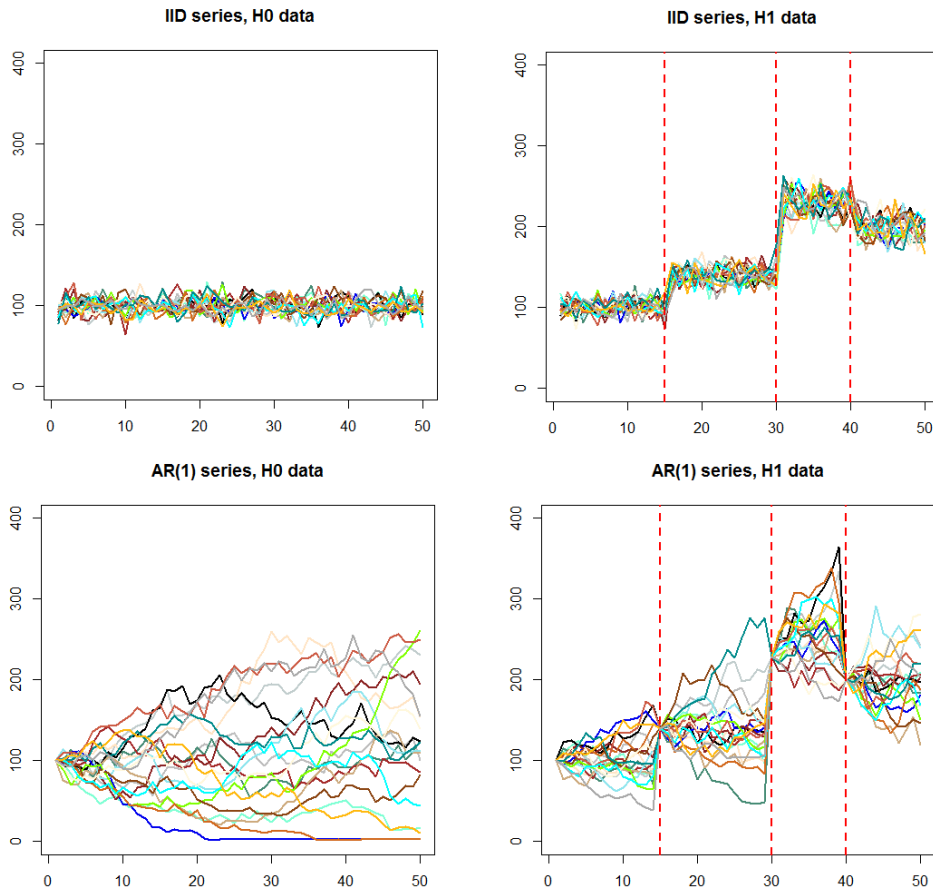


Figure 3: Simulated time series - iid vs AR(1) data

			MODEL 1		MODEL 2		MODEL 3		MODEL 4	
			BF	PT	BF	PT	BF	PT	BF	PT
IID	H ₀	$\lambda=1$	$\alpha=0$	$\alpha \leq 0.05$	$\alpha=0$	$\alpha \leq 0.05$	$\alpha=0$	$\alpha \leq 0.1$	$\alpha=0$	$\alpha \leq 0.1$
		$\lambda_2=2$	$\beta=1$	$\beta=1$	$\beta=1$	$\beta=1$	$\beta=1$	$\beta=1$	$\beta=0$	$\beta=1$
	H ₁	$\lambda_2=1.2$	$\beta=1$	$\beta=1$	$\beta=1$	$\beta=0.98$	$\beta=0$	$\beta=0.34$	$\beta=0$	$\beta=0.3$
multiple		$\beta=1$	$\beta=1$	$\beta=0.99$	$\beta=1$	$\beta=0$	$\beta=0.93$	$\beta=0$	$\beta=0.26$	
AR(1)	H ₀	$\lambda=1$	$\alpha=0.96$	$\alpha=0.66$	$\alpha=0.38$	$\alpha=0.24$	$\alpha=0.15$	$\alpha=0.26$	$\alpha=0$	$\alpha=0.18$
		$\lambda_2=2$	$\beta=1$	$\beta=0.97$	$\beta=0.81$	$\beta=0.75$	$\beta=0.53$	$\beta=0.81$	$\beta=0$	$\beta=0.52$
	H ₁	$\lambda_2=1.2$	$\beta=1$	$\beta=0.73$	$\beta=0.43$	$\beta=0.36$	$\beta=0.19$	$\beta=0.54$	$\beta=0$	$\beta=0.37$
		multiple	----	$\beta=0.98$	----	$\beta=0.91$	----	$\beta=0.84$	----	$\beta=0.67$

Figure 4: Simulation results - type I and II errors

H ₀ correct result	False positive
False negative	H ₁ correct result

BF PERFORMANCE (%)		PT PERFORMANCE (%)	
81.38	18.63	79.75	20.25
43.79	56.21	23.92	76.08

Figura 5: Simulation results - type I and II errors - summary

			MODEL 1		MODEL 2		MODEL 3		MODEL 4	
			BF	PT	BF	PT	BF	PT	BF	PT
IID	H ₀	$\lambda=1$	0	0	0	0	0	0	0	0
		$\lambda_2=2$	1	1	1	1	1	1	0	1
	H ₁	$\lambda_2=1.2$	1	1	1	1	0	0	0	0
		multiple	3	3	3	3	0	2	0	0
AR(1)	H ₀	$\lambda=1$	0	0	0	0	0	0	0	0
		$\lambda_2=2$	1	1	1	1	1	1	0	1
	H ₁	$\lambda_2=1.2$	1	1	0	0	0	1	0	0
		multiple	----	3	----	3	----	3	----	3

Figura 6: Simulation results - Number and position of detected change points

			MODEL 1		MODEL 2		MODEL 3		MODEL 4	
			BF	PT	BF	PT	BF	PT	BF	PT
IID	H ₀	$\lambda=1$	1	1.01	1	1.01	0.99	1	1	1
		$\lambda_1=1, \lambda_2=2$	0.99 - 2.00	1.04 - 2.00	1.00 - 2.00	1.04 - 2	0.99 - 2	1 - 2	1.5	1 - 2
	H ₁	$\lambda_1=1, \lambda_2=1.2$	1.00 - 1.20	1.01 - 1.20	1.00 - 1.20	1.01 - 1.2	1.09	1.1	1.1	1.1
		$\lambda_1=1, \lambda_2=1.4$ $\lambda_3=2.3, \lambda_4=2$	1.00 - 1.40 2.17 - 2.07	1.00 - 1.38 2.22 - 2.05	1.01 - 1.40 2.12 - 2.10	1.00 - 1.38 2.15 - 2.08	1.58	1.20 - 1.50 2.20	1.51	1.60
AR(1)	H ₀	$\lambda=1$	0.99	1.01	0.96	0.99	0.92	0.98	0.87	0.98
		$\lambda_1=1, \lambda_2=2$	1.05 - 2.04	1.05 - 2.03	1.09 - 2.10	1.11 - 2.05	1.18 - 1.90	1.08 - 1.99	1.41	1.20 - 1.78
	H ₁	$\lambda_1=1, \lambda_2=1.2$	1.01 - 1.14	1.01 - 1.14	1.06	1.06	1.1	1.01 - 1.18	1.07	1.09
		$\lambda_1=1, \lambda_2=1.4$ $\lambda_3=2.3, \lambda_4=2$	----	1.02 - 1.40 2.22 - 2.07	----	1.07 - 1.38 2.14 - 2.04	----	1.10 - 1.42 2.18 - 2.08	----	1.15 - 1.41 2.03 - 1.97

Figura 7: Simulation results - Time segment intensity estimates

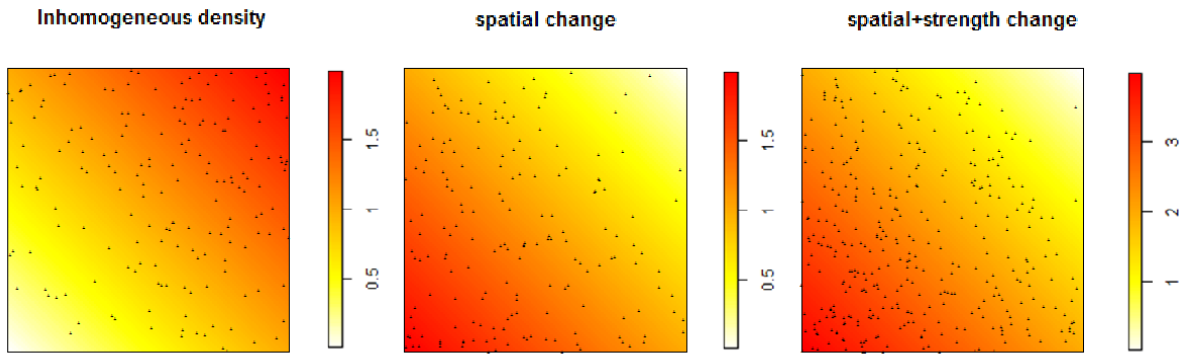


Figure 8: Spatial change - examples of simulated data

		MODEL 1		MODEL 2		MODEL 3		MODEL 4	
		BF	PT	BF	PT	BF	PT	BF	PT
SPATIAL CHANGE	Type II error	$\beta=0.38$	$\beta=0.44$	$\beta=0.42$	$\beta=0.26$	$\beta=1$	$\beta=1$	$\beta=1$	$\beta=1$
	Changepoint location	No chp	No chp	No chp	No chp	24	24	24	24
	Intensity estimate	0.95	0.95	0.97	0.97	1.05 - 1.00	1.03 - 1.01	1.06 - 1.02	1.04 - 1.00
SPATIAL AND SCALE CHANGE	Type II error	$\beta=1$	$\beta=1$	$\beta=1$	$\beta=1$	$\beta=1$	$\beta=1$	$\beta=1$	$\beta=1$
	Changepoint location	24	24	24	24	24	24	24	24
	Intensity estimate	1.00 - 1.95	1.00 - 1.95	0.99 - 1.96	0.99 - 1.97	1.06 - 2.00	1.01 - 2.00	1.03 - 2.01	1.02 - 2.00

Figure 9: Spatial change - summary of the results

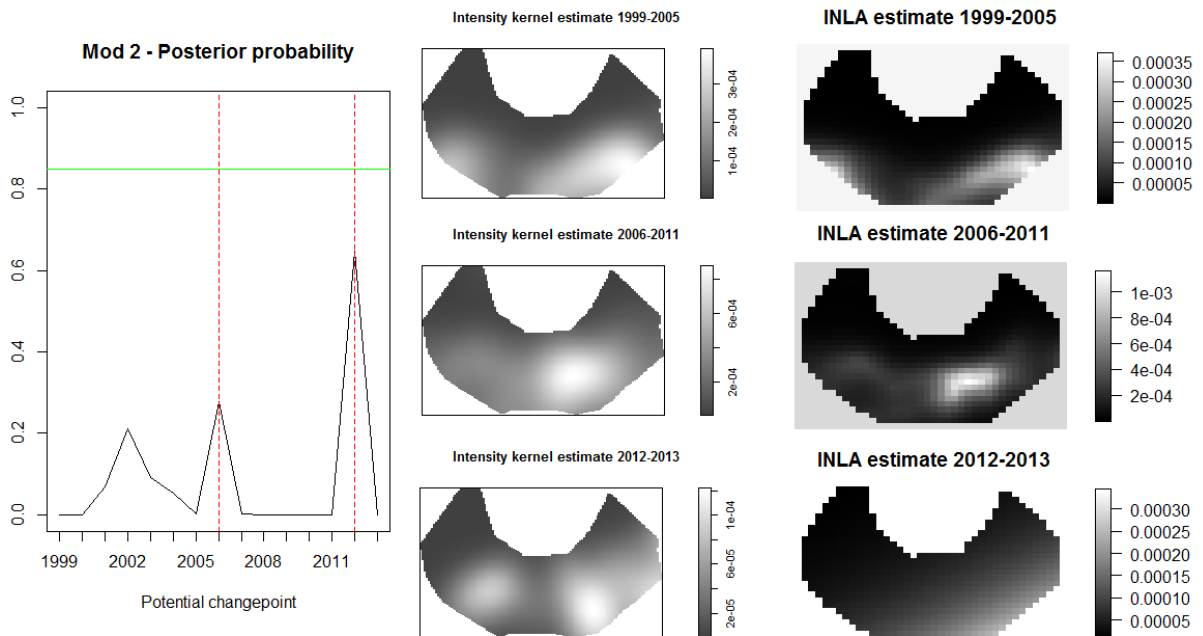


Figure 10: Spatial model and PT method - results